Supporting information

Near-infrared quantum dot and ^{89}Zr dual-labeled nanoparticles for in vivo Cerenkov imaging

Yiming Zhao,[1,2] Travis M. Shaffer,[2,3,4] Sudeep Das,[2] Carlos Pérez-Medina,[1] Willem J.M. Mulder,[1,5 *] and Jan Grimm[2,3 *]

1. Translational and Molecular Imaging Institute, Icahn School of Medicine at Mount Sinai, New York, New York 10029, United States
2. Molecular Pharmacology Program, Memorial Sloan-Kettering Cancer Center, New York, New York 10065, USA
3. Department of Radiology, Memorial Sloan Kettering Cancer Center, New York, New York 10065, United States
4. Department of Chemistry, Hunter College and the Graduate Center of the City University of New York, New York, New York 10065, United States
5. Department of Medical Biochemistry, Academic Medical Center, Amsterdam, 1105 AZ, The Netherlands

* Corresponding authors: grimmj@mskcc.org & willem.mulder@mssm.edu

Supporting Figures

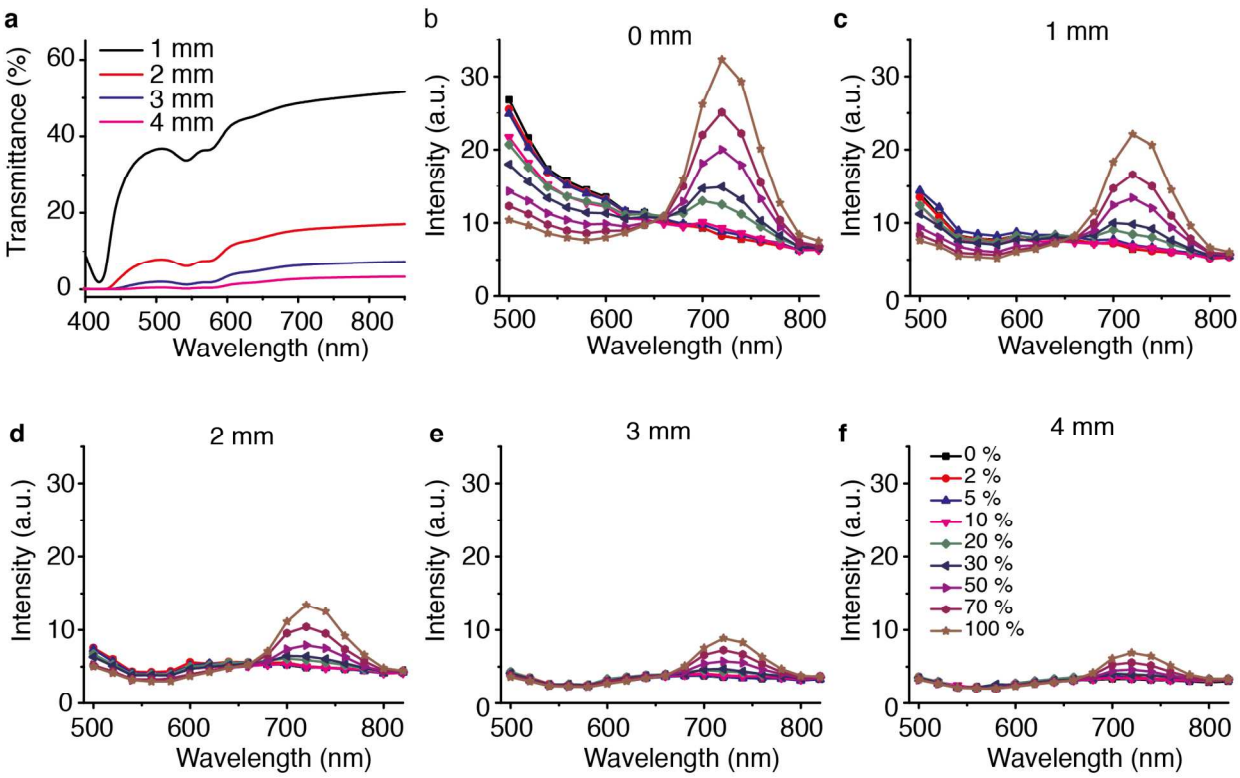

Figure S1. Spectral analysis on tissue phantom experiments. **a**, Absorption spectra of tissue phantoms with indicated thickness. **b-f,** Cerenkov emission spectra of transmitted light from mixtures of ^{89}Zr oxalate and Quantum dots (QDs) at different dilutions under tissue thicknesses of 0 mm (**b**), 1 mm (**c**), 2 mm (**d**), 3 mm (**e**), 4 mm (**f**).

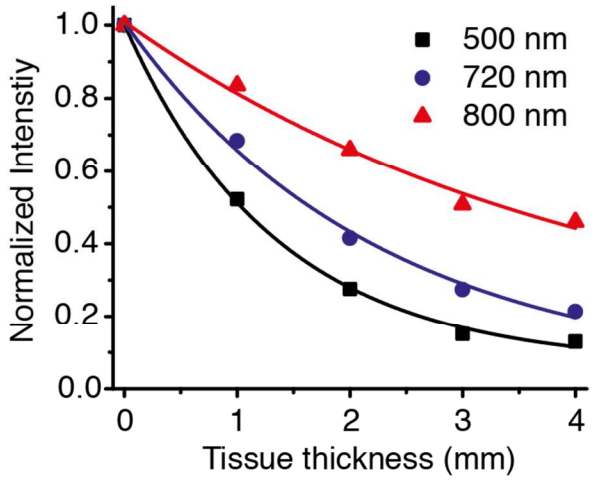

Figure S2. Intensity of transmitted light at different wavelengths and tissue thicknesses.

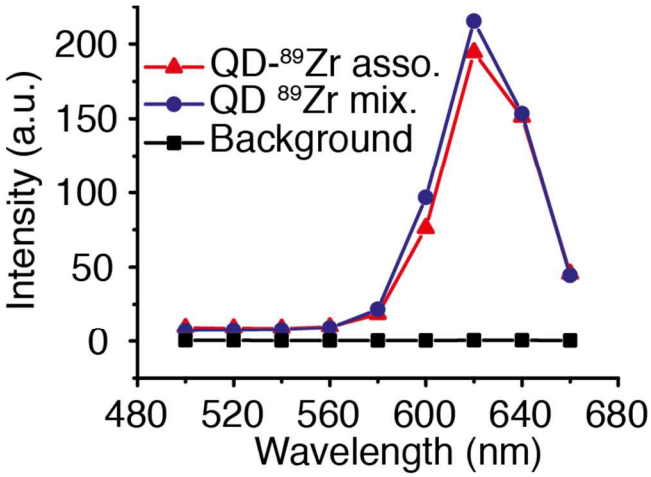

Figure S3. Comparison of the emission spectra of ^{89}Zr-QD-MC and a mixture of QD micelle and free ^{89}Zr oxalate solution at the same concentration of QD and radioactivity.

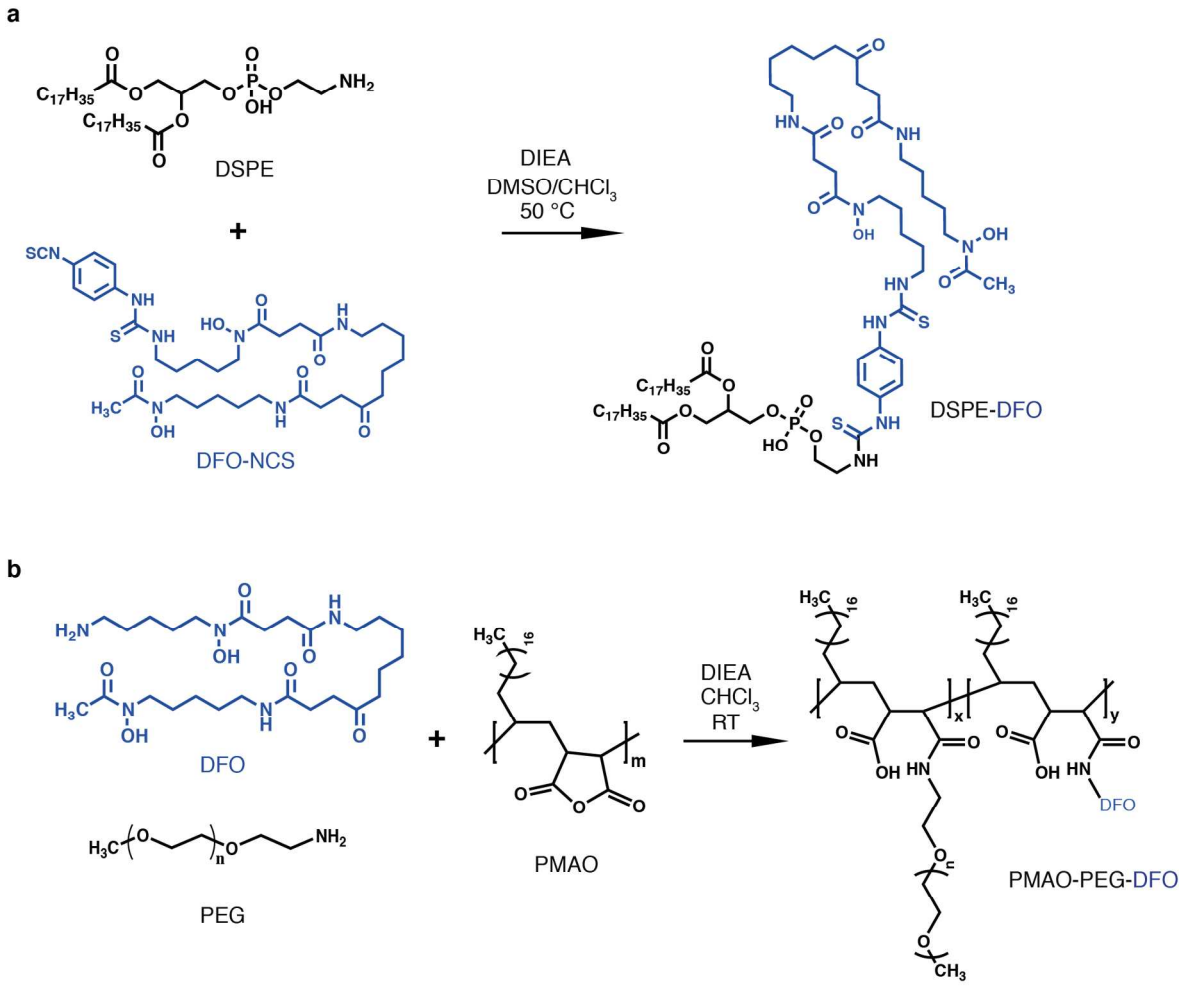

Figure S4. Synthesis of (**a**) DSPE-DFO, and (**b**) PMAO-PEG-DFO block copolymer.

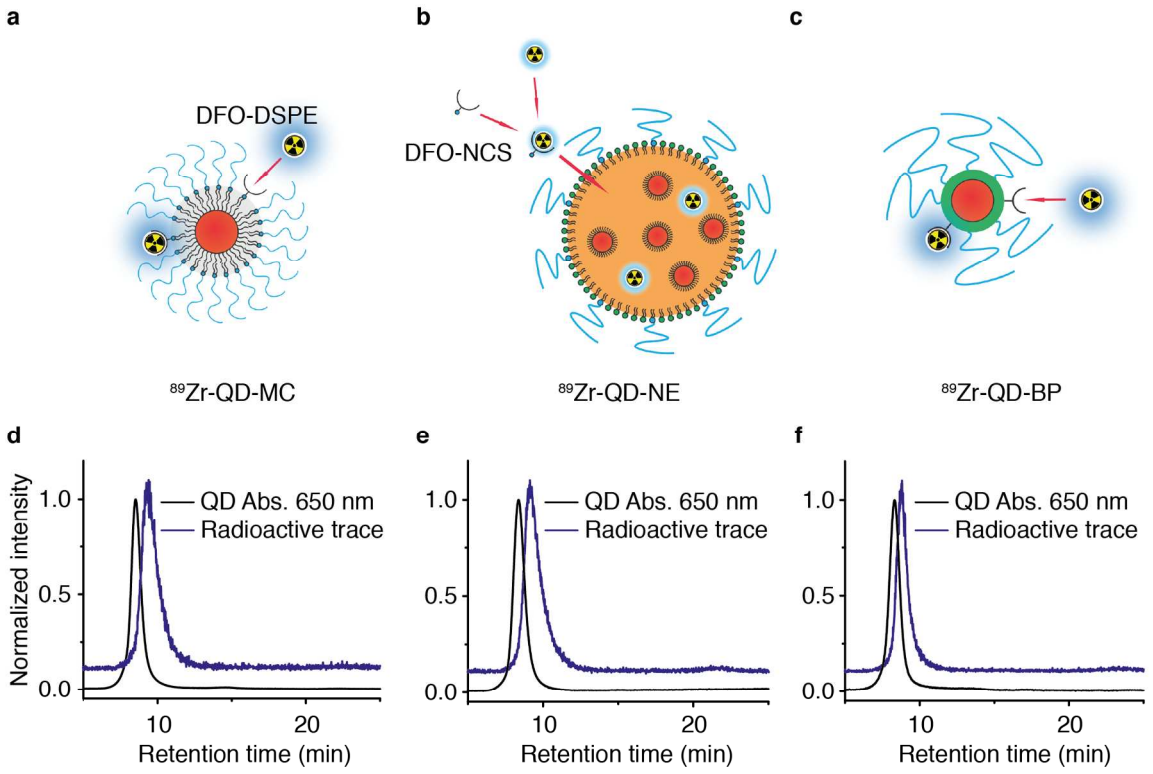

Figure S5. Schematic illustrations of NP radiolabeling (**a**-**c**) and HPLC chromatograms showing co-elution of QDs and radioactivity (d-f) for ^{89}Zr-QD-MC (**a**, **d**), ^{89}Zr-QD-NE (**b**, **e**), and ^{89}Zr-QD-BP (**c**, **f**).

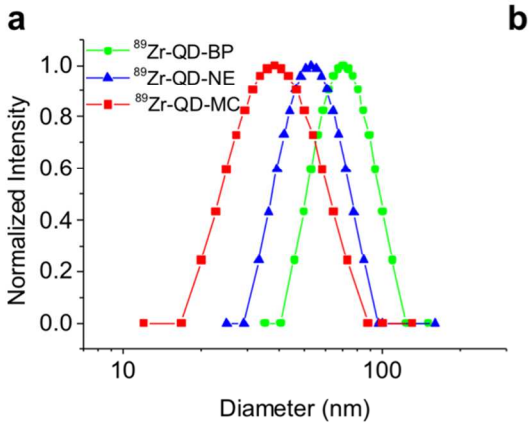

NPs	Mean Diameter (nm)	PDI	Zeta Potential (mV)
^{89}Zr-QD-MC	43.4±0.3	0.31	-17.2
^{89}Zr-QD-NE	56.7±0.6	0.16	-16.6
^{89}Zr-QD-BP	74.6±0.3	0.14	-12.3

Figure S6. a, Hydrodynamic size of dual-labeled NPs determined through dynamic light scattering (DLS). **b,** Mean diameter weighted by number, polydispersity index (PDI) and zeta potential of the different NPs.

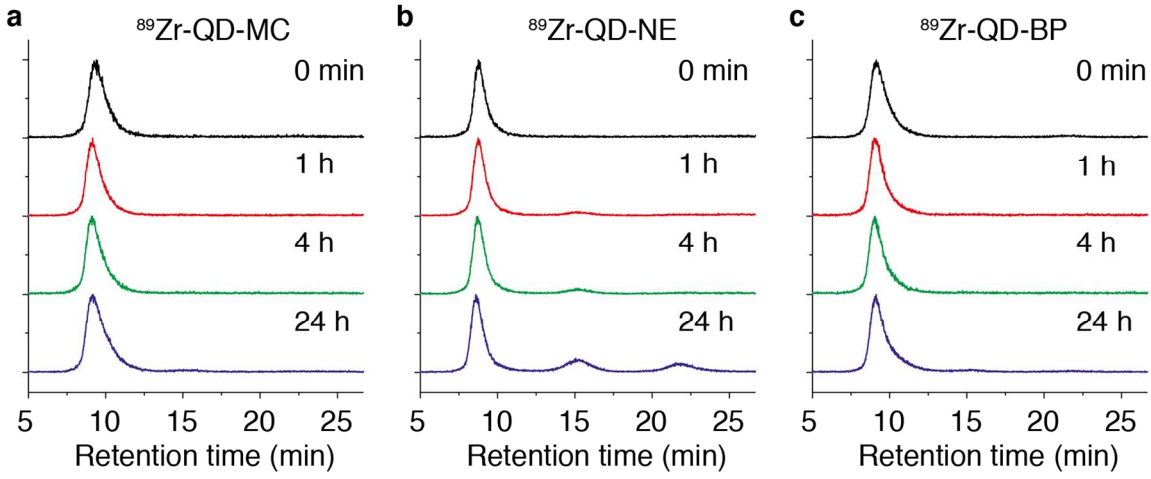

Figure S7. Serum stability of dual-labeled nanoparticles. Size exclusion chromatograms showing the radioactive trace for ^{89}Zr-QD-MC (**a**), ^{89}Zr-QD-NE (**b**), and ^{89}Zr-QD-BP (**c**) after incubation with fetal bovine serum for 0 min, 1, 4, and 24 h.

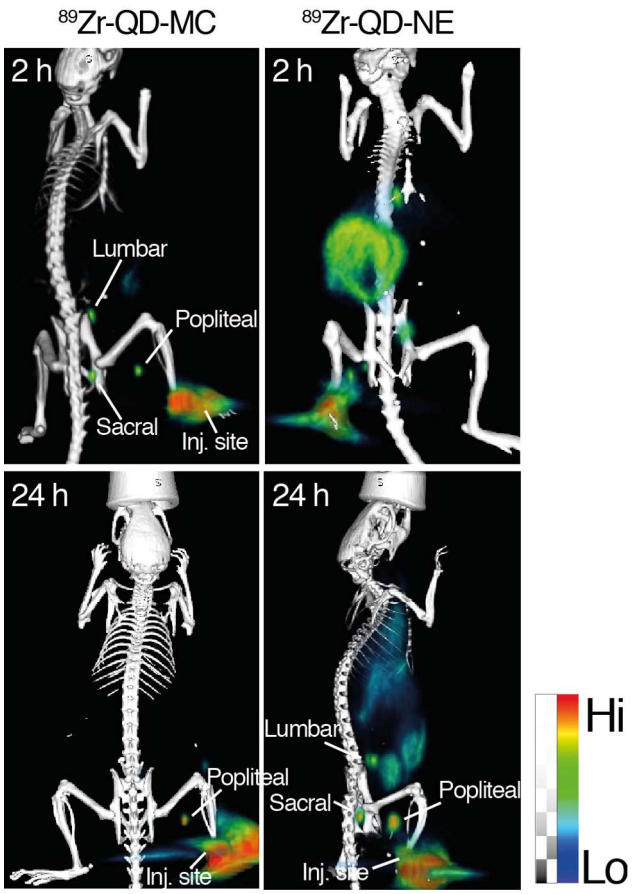

Figure S8. Lymph node PET/CT imaging using ^{89}Zr-QD-MC and ^{89}Zr-QD-NE at 2 and 24 h after footpad injection.

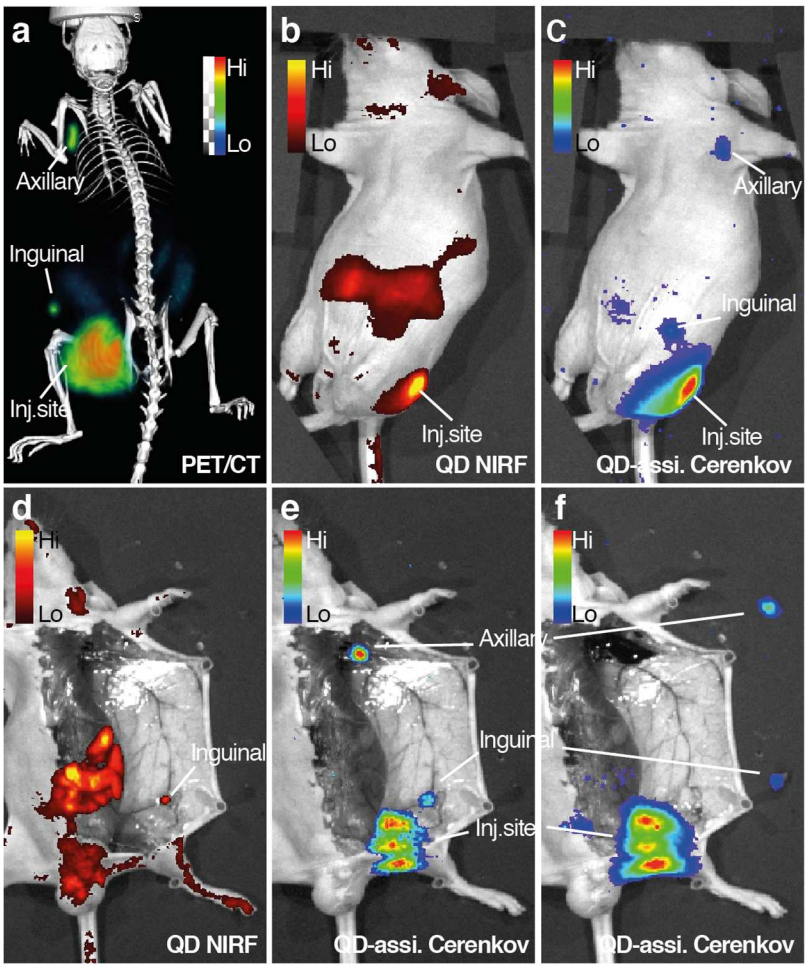

Figure S9. Sentinel lymph node multimodality imaging and subsequent Cerenkov imaging-guided lymph node removal using ^{89}Zr-QD-NE at 24 h post peri-tumoral injection.

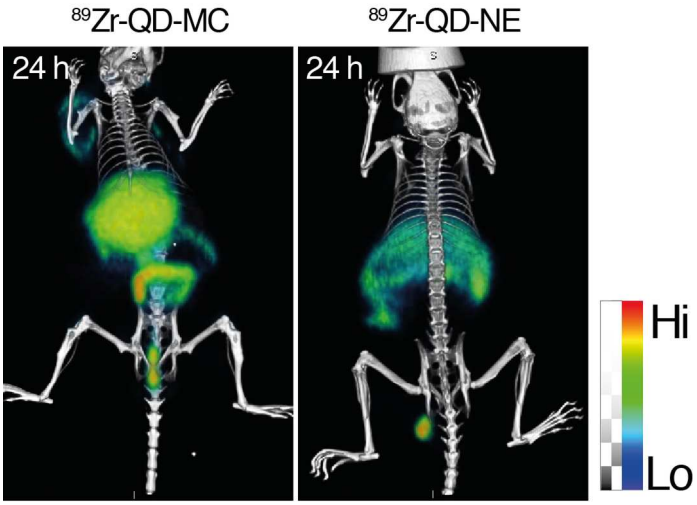

Figure S10. PET/CT images of tumor bearing mice at 24 h post-injection of ^{89}Zr-QD-MC (left) or ^{89}Zr-QD-NE (right). The former image showed hepatobiliary clearance of radioactive component from the ^{89}Zr-QD-MC, and the later one showed renal clearance of radioactive component from the ^{89}Zr-QD-NE